TUM

TECHNISCHE UNIVERSITÄT MÜNCHEN
INSTITUT FÜR INFORMATIK

A Cartesian-Space Method for Calculating Human Reachable Occupancy

Aaron Pereira and Matthias Althoff

TUM-I1759

A Cartesian-Space Method for Calculating Human Reachable Occupancy

Aaron Pereira[1] and Matthias Althoff[1]

***Abstract*— In previous work, we calculated overapproximative sets of human arm positions using a kinematic parameterisation of the human arm, for use in a formally-verifying robot trajectory planner. This has the drawback that inverse kinematics calculations are computationally expensive. In this technical report, we present another method, not requiring inverse kinematics but using the maximum Cartesian accelerations, velocities and positions attainable by a human. This can offer significant computational advantage, which is critical for a real-time motion planning application.**

I. Introduction

Predicting the possible future spatial occupancy of a human is necessary in human-robot co-existence (HRC) for ensuring robots do not collide with humans when moving. In a formally verified robot motion planner such as [1] or [2], conservative predictions of the future occupancies of nearby humans can be verified against the desired robot path to generate motion which is guaranteed to respect a safety criterion.

Much human motion is predictable, especially in a factory setting where humans and robots may work together. Several probability-based approaches can predict movement of the human with high accuracy, for example Ding et al. [3] uses Hidden Markov Models to predict hand position in reaching tasks, where as Koppula and Saxena [4] take a more high-level approach, exploiting the affordances of nearby objects to infer the intended goal of human reaching motions. Mainprice and Berenson populate a voxel grid with the probability of future occupancy using a Gaussian Mixture Model; these probabilities then inform a motion planner.

Co-working scenarios, however, can become dangerous when a human performs unexpected movement such as reflex movements, which are not accounted for in probabilistic models. When accounting for *all* human motion, the main challenge is the speed and unpredictability of human movements, leading to very large possible future occupancies. Ragaglia et Al. [5] estimate future movement using a kinematic model of the upper body and some assumed dynamic limits on the model's velocities, scaling robot motion according to the distance to the reachable occupancy. In [6] the authors present a method to bound such occupancies by abstracting the arm to a simple kinematic model and considering the maximum joint positions, velocities and accelerations observed in a set of archetypal movements. From these parameters, reachability analysis is used to calculate the set of joint positions during a future time interval, from which the reachable occupancy in Cartesian space is calculated. Drawbacks of this kinematic-based approach are 1) the expensive inverse and forward kinematic calculations and 2) the resulting complex volume, which requires a complex collision-checking algorithm.

[1]Technische Universität München, Boltzmannstr. 3, 85748 Garching, Germany, Email: {aaron.pereira, althoff} @tum.de

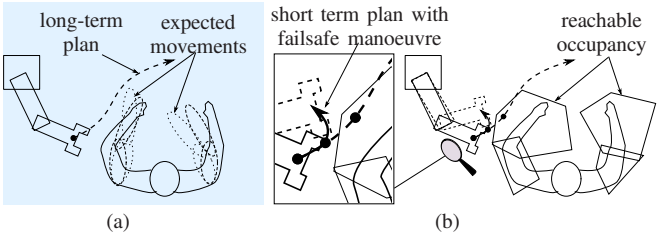

Fig. 1. (a) Long-term plan around expected human movement; (b) short-term plan with failsafe manoeuvre accounting for unexpected movement.

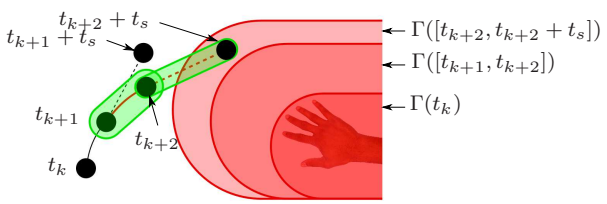

Fig. 2. Verifying safety of a short-term plan. The desired trajectory during time interval $[t_{k+1}, t_{k+2}]$ is determined to be unsafe, as the subsequent failsafe manoeuvre intersects the reachable occupancy $\Gamma([t_{k+1}, t_{k+2}])$. Hence we execute the failsafe manoeuvre verified in the previous timestep.

We present 3 fast, Cartesian-space methods for predicting human reachable occupancy which do not require kinematics. They can be used in parallel to form a tight occupancy for prediction of human movement up to arbitrary future times. In particular, this approach is useful in case of sensor failure and infrequent sensor updates.

In the next section we state the problem of reachable occupancy prediction in detail within the framework of a formally verified trajectory planner. Sec. III presents the models in detail and Sec. IV shows how they are parameterised. Some experimental validation is presented in Sec. V, and we conclude in Sec. VI.

II. Problem Statement

We consider a formally verified trajectory planner such as [1], [7]. The principle is that *no movement is executed without being previously verified safe*. At every point in time, we have a long-term trajectory (either predefined or planned around expected human movement as in [8], [7]) and a short-term plan, which consists of the currently executing section

of the long-term trajectory from t_k to t_{k+1}, followed by a *failsafe manoeuvre* until $t_{k+1} + t_s$. The failsafe manoeuvre brings the robot to a safe state, for example, a stationary state. This is illustrated in Fig. 1. Fig. 2 explains the online verification concept. While executing the current section, it is verified whether the next short term plan (from t_{k+1} to t_{k+2} on the long term trajectory followed by a failsafe manoeuvre) can be executed safely. If this is the case, the next section can be said to be *verified*, and the next short term plan is executed at time t_{k+1}. If not, the robot continues on the failsafe manoeuvre from the current short-term plan. Even while the failsafe manoeuvre is being executed, the robot can still plan and verify subsequent movements.

This type of trajectory planner needs an overapproximative prediction of the occupancy of set of positions of the human over the time interval of the short-term plan; such a prediction is called a *reachable occupancy* $\Gamma([t_i, t_f])$, defined as the entire set in space that the human arm could possibly occupy from initial time t_i until time horizon t_f. Since we assume no prior knowledge of the human's intention, this set is governed by the dynamics of the human arm and since these can be fast, $\Gamma([t_i, t_f])$ grows quickly as t_f increases. Hence critical to performance is a fast overapproximative model which gives as small a volume as possible while being conservative.

Below, we present the models to be evaluated and detail how the extreme movement data of the human is used to parameterise the models.

III. Methods for Calculation of Reachable Occupancy

A reachable occupancy from a kinematic model as in [1] or [5] is advantageous as it automatically exploits the rigid structure of the arm links and their coupling. However, inverse kinematics can be time consuming, and the conversion from a reachable set of joint angles to an occupancy in space is computationally expensive and creates a complex volume. We therefore present a simpler, fast-to-calculate Cartesian-space approach consisting of unions of simple capsules and spheres, which are easy to collision-check during verification against the planned path.

Since it is quicker to compute multiple simple, overapproximative models than one complex model, our approach uses three models using position, velocity and acceleration limits respectively, along with the current speed and velocity of the human, to compute the reachable occupancy. If the models are all overapproximative, the sets calculated according to them all include the *exact reachable occupancy* $\Gamma_{EX}([t_i, t_f])$, i.e. the set of all possible positions of the arm during time interval $[t_i, t_f]$. We therefore check all of these models against the occupancy of the robot along the short-term plan to be verified; if any of the reachable occupancies generated by these models are safe (i.e. do not collide with the robot), then the exact reachable occupancy is safe and the short-term plan is verified.

The arm is considered to be enclosed by two capsules, $\mathcal{C}_U$ running from the *shoulder* to the *elbow*, and $\mathcal{C}_F$ from the *elbow* to the *wrist*, and a sphere $\mathcal{S}_H$ centred on the *wrist*, as shown in Fig. 3a. The radius of $\mathcal{C}_U$ and $\mathcal{C}_F$ is taken as $0.1m$, and that of $\mathcal{S}_H$ is taken as $0.205m$ which is the 95$^{\text{th}}$ percentile length of British human hand [9]. In our implementation, the positions of the *shoulder*, *elbow* and *wrist* points were determined from infrared motion capture data of markers placed on the arm. Fig. 3b illustrates this. We next describe the novel Cartesian Space approaches to calculating the reachable occupancy.

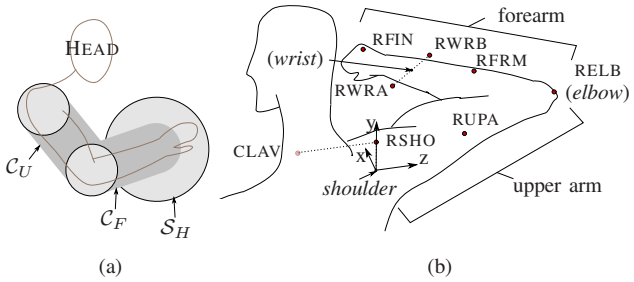

Fig. 3. (a) Enclosure of the arm in two capsules and a sphere, (b) Markers on the right arm and local base coordinate system. The *shoulder* point is taken as $40mm$ below RSHO, the *elbow* is at RELB and the *wrist* is taken as the midpoint of RWRA and RWRB.

A. Terminology

We first define some terminology and operators. Let $B(\mathbf{p}; r)$ be the closed ball of radius r centred at $\mathbf{p}$:

$$B(\mathbf{p}; r) = \{\mathbf{x} \mid \|\mathbf{x} - \mathbf{p}\| \leq r\}$$

A Sphere-Swept Volume (SSV) is the Minkowski sum of a polytope and a sphere (the Minkowski sum is defined on sets A and B as: $A \oplus B = \{a + b \,|\, a \in A, b \in B\}$). A capsule is an SSV where the polytope is a line segment. In the following models we often enclose two balls in another ball or a capsule, the operators for which we call BE and CE respectively. To define BE or CE on two balls $B(\mathbf{p}_1; r_1)$ and $B(\mathbf{p}_2; r_2)$, we must define the following terms:

$$\begin{aligned} &i = \texttt{indmax}(r_1, r_2), && j = \texttt{indmin}(r_1, r_2) \\ &\mathbf{x} = \mathbf{p}_i - \mathbf{p}_j, && \alpha = \max(r_i - r_j, \|\mathbf{x}\|) \\ &\beta = \min(r_i - r_j, \|\mathbf{x}\|) && \mathbf{p}_k = \mathbf{p}_j + \frac{\mathbf{x}}{\|\mathbf{x}\|} \cdot \beta \end{aligned}$$

The operators `indmax` and `indmin` return the indices of the maximum and minimum of the arguments. We can then define the operators:

$$\begin{aligned} &\text{BE}(B(\mathbf{p}_1; r_1), B(\mathbf{p}_2; r_2)) := B\Big(\frac{\mathbf{p}_i + \mathbf{p}_k}{2}; \frac{r_i + r_j + \alpha}{2}\Big), \\ &\text{CE}(B(\mathbf{p}_1; r_1), B(\mathbf{p}_2; r_2)) := \overline{\mathbf{p}_i, \mathbf{p}_k} \oplus B(\mathbf{0}; r_i), \end{aligned}$$

where $\mathbf{0} \in \mathbb{R}^3$ is the zero vector and $\overline{\mathbf{p}_i, \mathbf{p}_k}$ denotes the line segment between $\mathbf{p}_i$ and $\mathbf{p}_k$ Where one ball fully contains the other, i.e. $B(\mathbf{p}_j; r_j) \subset B(\mathbf{p}_i; r_i)$, then $\mathbf{p}_i = \mathbf{p}_k$.

In the following discussion, the subscripts *S, E, W, U, F* and *H* refer to the *shoulder, elbow, wrist, upper arm, forearm* and the *hand*.

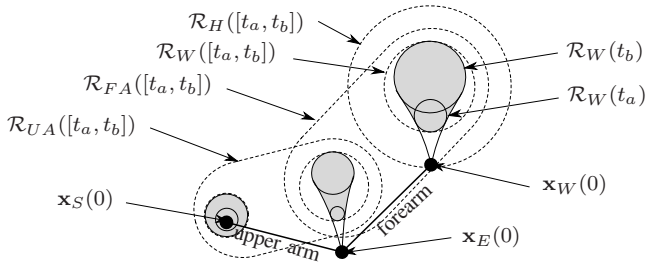

Fig. 4. Occupancy Γ_{ACC} of the human arm for time interval $[t_a, t_b]$ using the acceleration model.

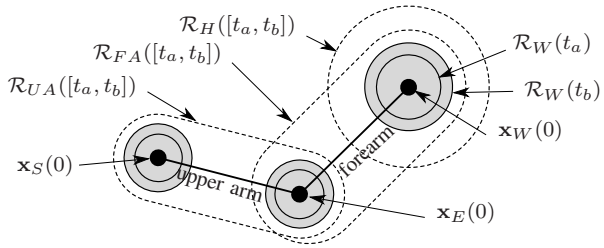

Fig. 5. Occupancy Γ_{VEL} of the human arm for time interval $[t_a, t_b]$ using the velocity model.

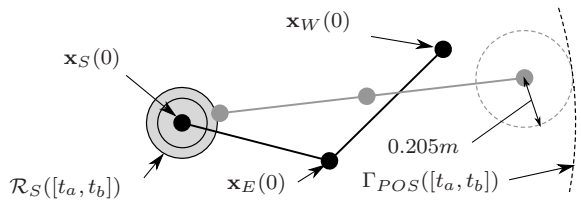

Fig. 6. Occupancy Γ_{POS} of the human arm for time interval $[t_a, t_b]$ using the position model.

B. Model of Acceleration Limits

Fig. 4 illustrates the acceleration model. The position of point $\mathbf{y}$ after time t is:

$$\mathbf{y}(t) = \mathbf{y}(0) + \dot{\mathbf{y}}(0) \cdot t + \int_0^t \int_0^{\tau'} \ddot{\mathbf{y}}(\tau) d\tau d\tau',$$

where $\mathbf{y}(0)$ and $\dot{\mathbf{y}}(0)$ are initial position and speed. Where $a_{\mathbf{y},\max}$ is the maximum magnitude of acceleration of $\mathbf{y}$, we consider that $\|\ddot{\mathbf{y}}\| \leq a_{\mathbf{y},\max}$, thus for the last term, $\int_0^t \int_0^{\tau'} \ddot{\mathbf{y}}(\tau) d\tau d\tau' \leq a_{\mathbf{y},\max} \frac{t^2}{2}$ holds. We let δy and $\delta \dot{y} \in \mathbb{R}$ be maximum measurement uncertainties in the position and velocity measurement; the reachable occupancy of a point $\mathbf{y} \in \mathbb{R}^3$ at time t according to the acceleration model is:

$$\mathcal{R}_{\mathbf{y}}(t) = B(\mathbf{y}(0); \delta y) \oplus B(\dot{\mathbf{y}}(0) \cdot t; \delta \dot{y} \cdot t) \oplus B(\mathbf{0}; \frac{a_{\max}}{2} \cdot t^2). \tag{1}$$

We obtain the reachable set of time interval $[t_a, t_b]$, denoted by $\mathcal{R}_y([t_a, t_b])$, by $\text{BE}(\mathcal{R}_y(t_a), \mathcal{R}_y(t_b))$. We omit the proof that this encloses the reachable set of the interval for brevity. In this way, we calculate the reachable sets of shoulder, elbow and wrist, $\mathcal{R}_S([t_a, t_b])$, $\mathcal{R}_E([t_a, t_b])$ and $\mathcal{R}_W([t_a, t_b])$. We omit time dependency for the rest of the derivation for clarity. The occupancy of the forearm $\mathcal{R}_F$ and of the upper arm $\mathcal{R}_U$ are capsules enclosing $\mathcal{R}_W$ and $\mathcal{R}_E$, and $\mathcal{R}_E$ and $\mathcal{R}_S$, respectively (by the property of convexity, the whole of the forearm and upper arm are included by enclosing their respective end points). $\mathcal{R}_F$ and $\mathcal{R}_U$ are extended by $0.1m$ to account for the arm thickness. As motivated above, the hand is inside a sphere centred on the wrist of radius $0.205m$. The reachable set of the hand $\mathcal{R}_H$ is therefore $\mathcal{R}_W$ extended by $0.205m$:

$$\begin{aligned}
\mathcal{R}_U([t_a,t_b]) &= \text{CE}(\mathcal{R}_S([t_a,t_b]), \mathcal{R}_E([t_a,t_b])) \oplus B(\mathbf{0}; 0.1), \\
\mathcal{R}_F([t_a,t_b]) &= \text{CE}(\mathcal{R}_E([t_a,t_b]), \mathcal{R}_W([t_a,t_b])) \oplus B(\mathbf{0}; 0.1), \\
\mathcal{R}_H([t_a,t_b]) &= \mathcal{R}_W([t_a,t_b]) \oplus B(\mathbf{0}, 0.205).
\end{aligned} \tag{2}$$

Γ_{ACC} is the union of two capsules and a sphere:

$$\Gamma_{ACC}([t_a,t_b]) = \mathcal{R}_F([t_a,t_b]) \cup \mathcal{R}_U([t_a,t_b]) \cup \mathcal{R}_H([t_a,t_b]).$$

C. Model of Velocity Limits

Although the acceleration model is usually accurate, when the human is moving near to its maximum velocity, the acceleration model does not consider that the human cannot accelerate further in the direction of motion, and will include some areas which are not reachable. A model based on velocity limits can account for this. The model of velocity limits is similar to that of acceleration limits:

$$\mathbf{y}(t) = \mathbf{y}(0) + \int_0^t \dot{\mathbf{y}}(\tau) d\tau$$

We consider $\dot{\mathbf{y}} \leq v_{\mathbf{y},\max}$, in which case $\int_0^t \dot{\mathbf{y}}(\tau) d\tau \leq v_{\mathbf{y},\max} \cdot t$. Then (1) becomes:

$$\mathcal{R}_{\mathbf{y}}(t) = B(\mathbf{y}(0); \delta y + v_{\mathbf{y},\max} \cdot t), \tag{3}$$

where $v_{\mathbf{y},\max}$ is the maximum velocity. As can be seen from Fig. 5, the reachable occupancy strictly encloses previous reachable occupancies, so $\Gamma_{VEL}([t_a, t_b]) = \Gamma_{VEL}(t_b)$. The sets $\mathcal{R}_F([t_a, t_b])$, $\mathcal{R}_U([t_a, t_b])$ and $\mathcal{R}_H([t_a, t_b])$ are calculated as in (2), and similarly:

$$\Gamma_{VEL}([t_a,t_b]) = \mathcal{R}_F([t_a,t_b]) \cup \mathcal{R}_U([t_a,t_b]) \cup \mathcal{R}_H([t_a,t_b]).$$

D. Model of Position Limits

The aforementioned models do not consider that body parts do not change in length and the extension of the reachable set from the shoulder cannot be more than the length of the outstretched arm. That is, the entire arm's workspace is within a ball whose radius is the length of the arm, and centred at the shoulder. Pathologically, we know that the reachable occupancy lies within the arm workspace, so this ball is an overapproximative set enclosing the exact reachable occupancy and hereby our simplest model. The lengths of the arm segments are the distances from shoulder to elbow and elbow to wrist, plus $0.205m$, as motivated earlier in this section. The ball is centered on the shoulder, the position of which we model using the velocity model

from (3), i.e. $\mathbf{x}_S(t) \in B(\mathbf{x}_S(0), v_{S,\max} \cdot t)$. See Fig. 6.

$$\Gamma_{POS}([t_a, t_b]) = B(\mathbf{x}_S(0); v_{S,\max} \cdot t + \|\mathbf{x}_S(0) - \mathbf{x}_E(0)\| + \|\mathbf{x}_E(0) - \mathbf{x}_W(0)\| + \delta y + 0.205)$$

IV. Data Collection and Parametrisation of Model

The parameters of maximum velocity and acceleration of the parts of the shoulder, elbow and wrist, $v_{S,\max}$, $v_{E,\max}$, $v_{W,\max}$, $a_{S,\max}$, $a_{E,\max}$ and $a_{W,\max}$, must represent the maxima attained over all movement that can occur in a HRC scenario.

Overapproximative prediction of human movement relies on capturing accurate data on the limits of human motion. We therefore captured infrared motion capture data from a representative range of humans performing several movements. 38 test subjects (12 female, 26 male) aged between 18 and 49 years, performed punching and sideways-sweeping movements as fast as possible; these movements were designed to resemble possible reflex movements or unexpected motions in a production line environment. Motion capture was at $120Hz$ and simple distance checks between markers were used to detect and ignore timesteps where the tracking system failed to correctly track relevant markers.

Offline, we simultaneously filter the data and extract the velocity and accelerations using a Kalman filter. The state of the system for the filter is the marker coordinates, their velocities and their accelerations. The error covariance was a diagonal matrix of $0.0001m$ and the process covariance was a diagonal matrix of zeros for the position and velocity parts of the state and $500ms^{-2}$ for the acceleration part, which adequately removes noise without attenuating accelerations.

The maximum velocity and acceleration magnitudes at the shoulder, elbow and wrist, $v_{S,\max}$, $v_{E,\max}$, $v_{W,\max}$, $a_{S,\max}$, $a_{E,\max}$ and $a_{W,\max}$, are found directly from the obtained velocities and accelerations of the shoulder, elbow and wrist points, $\dot{\mathbf{x}}_S$, $\dot{\mathbf{x}}_E$, $\dot{\mathbf{x}}_W$, $\ddot{\mathbf{x}}_S$, $\ddot{\mathbf{x}}_E$ and $\ddot{\mathbf{x}}_W$.

V. Evaluation

We evaluate the approach on a publicly available dataset from the Graphics Lab at Carnegie Mellon University[1]. In a previous work [6], we used an extensive dataset and classified movements into *Everyday*, *Sport*, *Dance* and *Acrobatics* movements. Here we use a subset of this and list the exact subjects and movements used for clarity, because *Acrobatics* movements from the previous dataset would not be found in industrial scenarios, and certain *Everyday* movements were also unrealistic for human-robot co-operation scenarios.

Our datasets are:

1) subject 62: construction work/random (25 motions);
2) subject 70: carrying a suitcase; (10 motions)
3) subject 80: everyday motions (44 motions);
4) subject 82: jumping, pushing, banging (10 motions);
5) subject 76: swatting at bug (1 motion);
6) subject 94, Indian dance (16 motions);
7) subject 102, basketball (32 motions);
8) subject 124, sport-related motions (13 motions)

[1]Available `mocap.cs.cmu.edu`, accessed 11.08.15.

TABLE I
Checks of overapproximation for 8 datasets

Dataset	Γ_{ACC}	Γ_{VEL}	Γ_{POS}
1 (25 motions)	25	25	25
2 (10 motions)	10	10	10
3 (44 motions)	44	44	44
4 (10 motions)	10	10	10
5 (1 motion)	1	1	1
6 (16 motion)	16	16	16
7 (32 motion)	**31**	32	32
8 (13 motion)	**9**	13	13

TABLE II
Volume comparison over a sample of data (m^3)

Prediction interval (ms)	Γ_{ACC}	Γ_{VEL}	Γ_{POS}
$[8.3, 16.7]$	0.08	0.44	2.05
$[25.0, 33.3]$	0.22	1.51	2.39
$[41.7, 50.0]$	0.67	3.87	2.76
$[58.3, 66.7]$	2.23	7.98	3.17

The first 5 were similar to movements expected at a workstation, and the last 3 were to test the limits of the prediction. For every timestep of every movement and for both arms we check whether the reachable occupancy during a time interval $[t_i, t_f]$ encloses the arm – in this case, all the markers on the arm at time t_f. From a sample of the data, we measure the average volume (volume calculations take too long to perform on all data). Position uncertainty is estimated at $0.01m$ and velocity uncertainty at $0.1ms^{-1}$. The time intervals we test are $[t_i, t_f] = [8.3, 16.7]; [25.0, 33.3]; [41.7, 50.0]$ and $[58.3, 66.7]$ (times in ms)[2]. In Tab. I, measurements are said to be included only if all markers at t_f are always included in the prediction for each time interval tested, for both arms. As can be seen in Tab. I, all approaches correctly account for all movement in the first 5 datasets, but not in datasets 6–8. The arm dynamics in dancing and sport movements may be faster than the dynamics in the data used to parameterise the model in Sec. IV, hence our assumptions do not hold.

The value Γ_{VEL} is always bigger than Γ_{ACC}. However, during high-speed movements near the velocity limit, Γ_{ACC} may include some volume which is actually not reachable, since the acceleration model does not consider velocity limits. Here Γ_{VEL} may be verified safe, meaning the trajectory is verified safe. Sometimes sensors may be obscured or may not update frequently. At times greater than $50ms$, both Γ_{VEL} and Γ_{ACC} become extremely large and could claim areas far from the shoulder as unsafe. Since Γ_{POS} models the constraint that the arm has a fixed total length, this could

[2]The test data was sampled at 60 and $120Hz$, so t_f corresponded to a whole number of timesteps in both.

TABLE III

COMPARISON OF PREDICTION TIMES (ALL VALUES ms)

Method	Method from [6]	Γ_{ACC}	Γ_{VEL}	Γ_{POS}
Time (averaged over all time intervals)	0.46	0.23	0.21	0.18

help verify the trajectory at larger time horizons. A projection of the reachable sets for Γ_{ACC} is shown in Fig. 7.

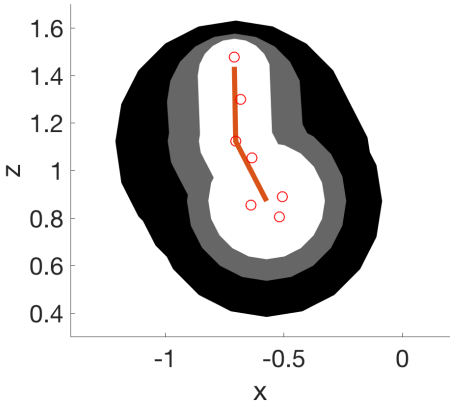

Fig. 7. Arm, shoulder at top and hand at bottom, underlaid with projections of reachable sets $\Gamma([8.3, 16.7]ms)$ in white, $\Gamma([25.0, 33.3]ms)$ in grey and $\Gamma([41.7, 50.0]ms)$ in black. Acceleration model; scale in metres

Computation times are shown in Tab. III. As can be seen, the approach from [6] using a kinematic arm model takes longer. Since the three approaches can be calculated in parallel, the overall time for calculation of the reachable occupancy may be shorter than the approach with a kinematic model.

VI. CONCLUSION

We present a Cartesian-space approach to predicting the human reachable occupancy in the context of a formally verifying path planner. The approaches work well in combination with each other, and since they are all overapproximative, the tightest approach at any time can be chosen. The approaches are computationally efficient enough to be used online within the context of an formally verified trajectory planner.

ACKNOWLEDGMENT

We gratefully acknowledge the work of Jonas Schmidtler, Thomas Illa and Asuman Sezgin, who captured the motion data and Natalie Reppekus for contribution to implementation. The comparison data used in this project was obtained from `mocap.cs.cmu.edu`; this database was created with funding from NSF EIA-0196217. The research leading to this article has received funding from the People Programme (Marie Curie Actions) of the European Union's Seventh Framework Programme FP7/2007-2013/ under REA grant agreement number 608022. The authors also gratefully acknowledge financial support by the European Commission project UnCoVerCPS under grant number 643921.

REFERENCES

[1] A. Pereira and M. Althoff, "Safety control of robots under computed torque control using reachable sets," in *Proc. of the IEEE Int. Conf. on Robotics and Automation*, 2015.

[2] S. Petti and T. Fraichard, "Safe Motion Planning in Dynamic Environments," in *Proc. of the IEEE-RSJ Int. Conf. on Intelligent Robots and Systems*, 2005.

[3] H. Ding, G. Reißig, K. Wijaya, D. Bortot, K. Bengler, and O. Stursberg, "Human arm motion modeling and long-term prediction for safe and efficient human-robot-interaction," in *Proc. 2011 IEEE Intl. Conf. Robotics and Automation (ICRA), Shanghai, China, 9-13 May 2011*. New York: IEEE, 2011, pp. 5875–5880. [Online]. Available: http://dx.doi.org/10.1109/ICRA.2011.5980248

[4] H. Koppula and A. Saxena, "Anticipating human activities using object affordances for reactive robotic response," *IEEE Trans. Pattern Anal. Mach. Intell.*, vol. 38, no. 1, pp. 14–29, 2015.

[5] M. Ragaglia, A. Zanchettin, and P. Rocco, "Safety-aware trajectory scaling for human-robot collaboration with prediction of human occupancy," in *Int. Conf. on Advanced Robotics*, 2015, pp. 85–90.

[6] A. Pereira and M. Althoff, "Overapproximative arm occupancy prediction for human-robot co-existence built from archetypal movements," in *Proc. IEEE/RSJ Int. Conf. on Intelligent Robots and Systems*, 2016, (accepted).

[7] M. J. Zeestraten, A. Pereira, M. Althoff, and S. Calinon, "Online motion synthesis with minimal intervention control and formal safety guarantees," in *Proc. of IEEE Systems, Man and Cybernetics*, 2016 (Accepted).

[8] J. Mainprice and D. Berenson, "Human-robot collaborative manipulation planning using early prediction of human motion," in *Proc. IEEE/RSJ Int. Conf. Intelligent Robots and Systems*, 2013, pp. 299–306.

[9] S. Pheasant and C. M. Haslegrave, *Bodyspace: Anthropometry, Ergonomics and the Design of Work*. Taylor & Francis CRC Press, 2006, ch. Hands and Handles, pp. 143–160.